

# Thermo-optical characteristics and concentration quenching effects in Nd<sup>3+</sup>-doped yttrium calcium borate glasses

D. R. S. Santos,<sup>1</sup> C. N. Santos,<sup>2,3</sup> A. S. S. de Camargo,<sup>2,a)</sup> W. F. Silva,<sup>1</sup> W. Q. Santos,<sup>1</sup> M. V. D. Vermelho,<sup>1</sup> N. G. C. Astrath,<sup>4</sup> L. C. Malacarne,<sup>4</sup> M. S. Li,<sup>2</sup> A. C. Hernandez,<sup>2</sup> A. Ibanez,<sup>3</sup> and C. Jacinto<sup>1,b)</sup>

<sup>1</sup>Grupo de Fotônica e Fluidos Complexos, Instituto de Física, Universidade Federal de Alagoas, 57072-970 Maceió - Al, Brazil

<sup>2</sup>Instituto de Física de São Carlos, Universidade de São Paulo, 13560-970 São Carlos - SP, Brazil

<sup>3</sup>Institut Néel, CNRS and Université Joseph Fourier, BP166, F38042 Grenoble Cedex 9, France

<sup>4</sup>Departamento de Física, Universidade Estadual de Maringá, Av. Colombo 5790, 87020-900, Maringá, PR, Brazil

(Received 14 January 2011; accepted 24 February 2011; published online 23 March 2011)

In this work we present a comprehensive study of the spectroscopic and thermo-optical properties of a set of samples with composition  $x\text{Nd}_2\text{O}_3-(5-x)\text{Y}_2\text{O}_3-40\text{CaO}-55\text{B}_2\text{O}_3$  ( $0 \leq x \leq 1.0$  mol%). Their fluorescence quantum efficiency ( $\eta$ ) values were determined using the thermal lens technique and the dependence on the ionic concentration was analyzed in terms of energy transfer processes, based on the Förster–Dexter model of multipolar ion–ion interactions. A maximum  $\eta = 0.54$  was found to be substantially higher than for yttrium aluminoborate crystals and glasses with comparable Nd<sup>3+</sup> content. As for the thermo-optical properties of yttrium calcium borate, they are comparable to other well-known laser glasses. The obtained energy transfer microparameters and the weak dependence of  $\eta$  on the Nd<sup>3+</sup> concentration with a high optimum Nd<sup>3+</sup> concentration put this system as a strong candidate for photonics applications. © 2011 American Institute of Physics. [doi:10.1063/1.3567091]

## I. INTRODUCTION

Yttrium borates in the ternary systems  $\text{Y}_2\text{O}_3\text{-Al}_2\text{O}_3\text{-B}_2\text{O}_3$  (YAB) and  $\text{Y}_2\text{O}_3\text{-CaO-B}_2\text{O}_3$  (YCOB) are very interesting nonlinear optical crystals with excellent chemical and physical properties.<sup>1</sup> When doped with the trivalent rare earth ions Nd<sup>3+</sup> and Yb<sup>3+</sup> they become potential systems for generation of CW and femtosecond-pulsed laser emission in the near-infrared spectral region,<sup>2–5</sup> and for self frequency doubling in the green.<sup>6,7</sup> Despite such interesting applications, the requirement of expensive and time consuming techniques for the growth of such crystals has led researchers to explore their glassy counterparts<sup>8–10</sup> for similar or new applications. Recently, we have reported on the luminescence and thermo-optical properties of Nd<sup>3+</sup>-doped  $\text{YAl}_3(\text{BO}_3)_4$  (YAlB) glasses with higher fluorescence quantum efficiency than the Nd:YAB crystal,<sup>9</sup> and on a detailed structural investigation of the glasses, and their corresponding vitroceraamics, as a function of compositional changes.<sup>11,12</sup> However, to the best of our knowledge, there have been no reports on the spectroscopic and thermo-optical characterization of undoped and Nd<sup>3+</sup>-doped  $\text{YCa}_4\text{O}(\text{BO}_3)_3$  (YCaB) glasses, which have been recently introduced by some of us.<sup>10,19</sup> A structural study of samples with compositions  $x\text{Y}_2\text{O}_3.8x\text{CaO}-(100-9x)\text{B}_2\text{O}_3$  ( $x = 4, 5, \text{ and } 6$  mol%), via Raman and infrared reflectance spectroscopies, has shown that the glasses contain a complex distribution of three-coordinated ortho and pyroborate groups and four-coordinated pentaborate groups, and as the CaO

addition increases there is a clear increase of the former.<sup>10</sup> It was also found that the composition with  $x = 5$  is the one that yields the most chemically and thermally stable glasses.

Given the attractiveness of higher flexibility in glass preparation, as compared to crystals, and the possibility of similar and new applications, a full structural and spectroscopic understanding of these new materials is required. With regard to the application as laser media, some very important issues to be addressed are the thermo-optical properties of the host and active ions, and concentration quenching effect due to nonradiative losses via energy migration (EM) and cross relaxations (CRs) between the ions. These features, mainly the latter, can strongly compromise the fluorescence quantum efficiency ( $\eta$ ) of the glasses. The experimental determination of the absolute value of  $\eta$  in luminescent solids is known to be a challenging task, due to the requirement of complicated experimental setups, the need of absolute photodetector calibration, the knowledge of absolute ion concentration, and a suitable standard sample. Alternatively, one method that has been successfully used for obtaining  $\eta$ , particularly for Yb<sup>3+</sup>- and Nd<sup>3+</sup>-doped transparent solids, is the normalized-lifetime thermal-lens (TL) method.<sup>13,14</sup> The method is based on measurements of the photothermal signals and the excited state lifetimes of a set of samples with the same host composition and varying ion concentration. Once  $\eta$  values are determined as a function of ion concentration, they can be effectively employed for the determination of the energy transfer microscopic parameters  $C_{DX}$  ( $X = D$  for donor–donor transfer as in EM, and  $X = A$  for donor–acceptor transfer, as in CRs). Among other systems, we have recently applied this methodology in the study

<sup>a)</sup>Electronic mail: andreasc@ifsc.usp.br.

<sup>b)</sup>Electronic mail: cjacinto@if.ufal.br.

TABLE I. Samples and Neodymium concentrations investigated.

Sample	Nd <sub>2</sub> O <sub>3</sub> (mol%)	Nd <sup>3+</sup> (10 <sup>20</sup> ions/cm <sup>3</sup> )
NYCaB10	0.10	0.3898
NYCaB25	0.25	0.9670
NYCaB35	0.35	1.3480
NYCaB50	0.50	1.9110
NYCaB75	0.75	2.8330
NYCaB100	1.00	3.7320

of fluorescence quenching effects in Nd<sup>3+</sup>-doped lead lanthanum zirconate titanate ferroelectric (Nd:PLZT) transparent ceramics for which the results agreed well with theoretical predictions.<sup>15</sup>

In this work we present a detailed spectroscopic and thermo-optical characterization of Nd:YCaB glasses with the same atomic ratio of the YCOB crystal ([Y]/[Ca] = 1/4) and 55 mol% boron oxide content. The experimental results are correlated to a theoretical approach,<sup>13,16–18</sup> aiming to identify and quantify nonradiative contributions responsible for the fluorescence quenching in this system. To this end we employ ground state absorption, steady-state/time-resolved luminescence, and the thermal lens technique in association with the Judd–Ofelt (JO) theory and the Förster–Dexter model for energy transfer.<sup>17</sup>

## II. EXPERIMENTAL PROCEDURE

The glass samples with composition  $x\text{Nd}_2\text{O}_3-(5-x)\text{Y}_2\text{O}_3-40\text{CaO}-55\text{B}_2\text{O}_3$  with  $0 \leq x \leq 1.0$  mol%, hereafter referred to as YCaB and NYCaB100x, were prepared by the conventional melt quenching method as previously described.<sup>10,19</sup> Table I presents their corresponding Nd<sup>3+</sup> concentration in mol% and ions cm<sup>-3</sup> used in this work. The amorphous nature and structural characterization of the samples were verified by x-ray diffraction and Raman and FT–IR spectroscopies (not shown). In the doping concentration range studied, the structural characteristics of the NYCaB100x samples are very similar to those of the undoped YCaB sample.<sup>10</sup> Ground state absorption was measured in a UV-VIS-NIR Cary 17 spectrometer in the range from 250 to 950 nm, and emission spectra were recorded using a diode laser (810 nm) as excitation source. The luminescent signals were dispersed by a 64 cm single-grated monochromator with 0.1 nm resolution, amplified by a lock-in, and collected by an S-20 photomultiplier. The <sup>4</sup>F<sub>3/2</sub> state lifetime values were obtained by analyzing the 1064 nm emission decay curves obtained using a Ge detector with rise time < 3 μs, comparable to the cut-off time of modulation. The thermal lens experiments were carried out in the dual beam mode-mismatched configuration<sup>20</sup> using an Ar<sup>+</sup> laser (514.5 nm) as the excitation source and a HeNe laser (632.8 nm) as the probe beam.

## III. RESULTS AND DISCUSSIONS

### A. Absorption, luminescence, and Judd-Ofelt analysis

The room temperature absorption coefficient spectrum of the NYCaB75 is presented in Fig. 1. Concerning line posi-

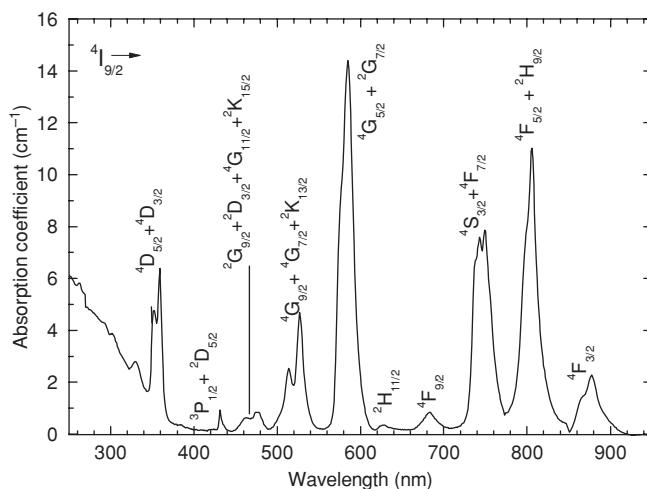


FIG. 1. Representative absorption spectrum of the NYCaB75 glass at room temperature.

tions and widths corresponding to transitions from the ground state <sup>4</sup>I<sub>9/2</sub> to the excited states of neodymium, the spectrum is representative for the other samples and resemble that of the Nd:YCOB crystal as well.<sup>21</sup> The linear dependence of the integrated area of the band at 800 nm (<sup>4</sup>I<sub>9/2</sub> → <sup>2</sup>H<sub>9/2</sub>, <sup>4</sup>F<sub>5/2</sub>) with Nd<sub>2</sub>O<sub>3</sub> concentration (not shown) indicates that the ionic incorporation was successful in the range studied, and it is in agreement with the nominal compositions. The UV edge of these glasses is around 240 nm, wider than in bismuth-borate glasses,<sup>22</sup> and the energy gap was calculated to be around 5.9 eV,<sup>19</sup> comparable to that of other glass compositions containing up to 80% boron oxide content.<sup>19,23</sup>

In Fig. 2, the representative luminescence spectrum of the NYCaB75 glass displays the three typical emissions from the emitting level <sup>4</sup>F<sub>3/2</sub> to the terminal levels <sup>4</sup>I<sub>9/2</sub>, <sup>4</sup>I<sub>11/2</sub>, and <sup>4</sup>I<sub>13/2</sub> of Nd<sup>3+</sup>, at 900, 1060, and 1320 nm, respectively. As it is common for Nd<sup>3+</sup>-doped systems, the transition to level <sup>4</sup>I<sub>15/2</sub> is not detected in this intensity scale due to its very small branching ratio (≈1%). The inset of the same figure presents the integrated intensity for the 1060 nm emission as

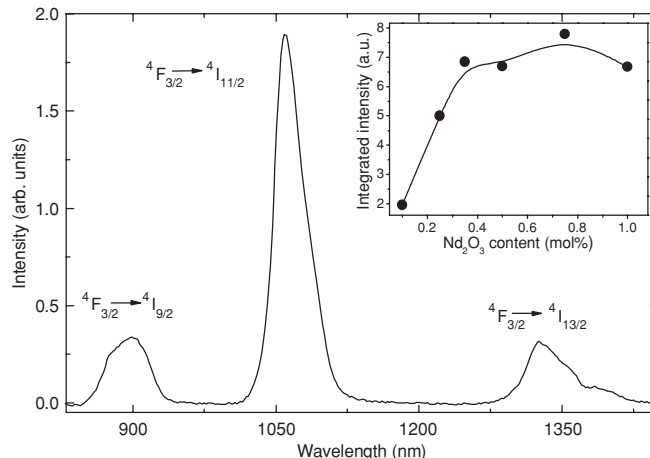


FIG. 2. Luminescence spectrum of the NYCaB75 glass at room temperature and  $\lambda_{\text{exc}} = 810$  nm. The inset presents the integrated intensity of the band at 1060 nm as a function of Nd<sub>2</sub>O<sub>3</sub> content.

TABLE II. Experimental and calculated Nd<sup>3+</sup> oscillator strength values for the NYCaB100x glasses.

Sample	Transition ( <sup>4</sup> I <sub>9/2</sub> → ...)	Wavelength (nm)	f <sub>exp</sub> (×10 <sup>-6</sup> )	f <sub>cal</sub> (×10 <sup>-6</sup> )	Error (%)
NYCaB10	(1) <sup>4</sup> F <sub>3/2</sub>	875.8	4.892	5.423	10.80
	(2) <sup>4</sup> F <sub>5/2</sub> , <sup>2</sup> H <sub>9/2</sub>	804.0	15.773	15.826	0.34
	(3) <sup>4</sup> F <sub>7/2</sub> , <sup>4</sup> S <sub>3/2</sub>	743.5	15.755	15.826	0.45
	(4) <sup>4</sup> G <sub>5/2</sub> , <sup>2</sup> G <sub>7/2</sub>	579.5	31.662	31.74	0.25
	(5) <sup>4</sup> G <sub>9/2</sub> , <sup>4</sup> G <sub>7/2</sub> , <sup>2</sup> K <sub>13/2</sub>	519.0	13.366	12.073	9.67
NYCaB35	(1) <sup>4</sup> F <sub>3/2</sub>	875.8	4.272	4.788	12.08
	(2) <sup>4</sup> F <sub>5/2</sub> , <sup>2</sup> H <sub>9/2</sub>	804.0	14.401	14.157	1.69
	(3) <sup>4</sup> F <sub>7/2</sub> , <sup>4</sup> S <sub>3/2</sub>	743.5	13.976	14.221	1.75
	(4) <sup>4</sup> G <sub>5/2</sub> , <sup>2</sup> G <sub>7/2</sub>	579.5	31.29	31.337	0.15
	(5) <sup>4</sup> G <sub>9/2</sub> , <sup>4</sup> G <sub>7/2</sub> , <sup>2</sup> K <sub>13/2</sub>	519.0	11.66	10.955	6.05
NYCaB75	(1) <sup>4</sup> F <sub>5/2</sub> , <sup>2</sup> H <sub>9/2</sub>	804.0	14.921	15.021	0.67
	(2) <sup>4</sup> F <sub>7/2</sub> , <sup>4</sup> S <sub>3/2</sub>	743.5	15.308	15.252	0.37
	(3) <sup>4</sup> F <sub>9/2</sub>	680.6	1.277	1.206	5.56
	(4) <sup>4</sup> G <sub>5/2</sub> , <sup>2</sup> G <sub>7/2</sub>	579.5	32.967	32.977	0.03
	(5) <sup>4</sup> G <sub>9/2</sub> , <sup>4</sup> G <sub>7/2</sub> , <sup>2</sup> K <sub>13/2</sub>	519.0	11.683	11.499	1.57

a function of Nd<sup>3+</sup> concentration showing a maximum for the NYCaB75 sample. For NY:CaB samples doped with up to 0.5 mol% the effective width of the 1060 nm band  $\Delta\lambda_{\text{eff}} = [\int I_{\text{lum}}(\lambda)d\lambda/I_{\text{lum}}(\lambda)_{\text{peak}}]$  (where  $I_{\text{lum}}(\lambda)$  is the emission intensity for the wavelength  $\lambda$  and  $I_{\text{lum}}(\lambda)_{\text{peak}}$  is the peak intensity) is 36 nm whereas for the NYCaB75 and NYCaB100 it is 38 nm. This slight, but consistent, increase might be an indication that for these concentrations and higher ones, a fraction of Nd<sup>3+</sup> ions occupy Ca<sup>2+</sup> environments in addition to those of Y<sup>3+</sup>. In Nd<sub>x</sub>La<sub>2-x</sub>B<sub>10</sub>O<sub>19</sub> crystals, inequivalent Nd<sup>3+</sup> environments were evidenced for  $x > 0.036$  (0.25 mol%),<sup>24</sup> as well as in Nd<sup>3+</sup> or Yb<sup>3+</sup> doped YCOB and GdCa<sub>4</sub>O(BO<sub>3</sub>)<sub>3</sub> (GdCOB) crystals.<sup>25,26</sup>

On the basis of the ground state absorption and the luminescence spectra of three samples (0.10, 0.35, and 0.75 mol%), the radiative properties of the NYCaB100x glasses were evaluated via the Judd-Ofelt formalism.<sup>27</sup> These parameters were obtained by solving a system of equations from the five main absorption bands, as indicated in Table II, where we compare the experimental and calculated oscillator strengths of these bands. The obtained values of the phenomenological intensity parameters  $\Omega_2$ ,  $\Omega_4$ , and  $\Omega_6$  are presented in Table III, with average values of  $\Omega_2 = 5.25 \times 10^{-20}$ ,  $\Omega_4 = 9.60 \times 10^{-20}$ , and  $\Omega_6 = 9.87 \times 10^{-20}$  cm<sup>2</sup>. These values are much larger than those of Nd:YCOB (Ref. 21) and slightly larger than those of Nd<sup>3+</sup>-doped yttrium – aluminoborate (NYAB) glasses and crystals.<sup>9,28</sup> The average radiative lifetime ( $\tau_{\text{rad}}$ ) value of the emitting level <sup>4</sup>F<sub>3/2</sub> is 150  $\mu$ s (Table IV), relatively smaller than that of Nd:YAIB glass,<sup>21</sup>

TABLE III. Phenomenological JO intensity parameters for NYCaB100x glasses for three Nd<sup>3+</sup> concentrations.

Sample	$\Omega_2$ (×10 <sup>-20</sup> cm <sup>2</sup> )	$\Omega_4$ (×10 <sup>-20</sup> cm <sup>2</sup> )	$\Omega_6$ (×10 <sup>-20</sup> cm <sup>2</sup> )
NYCaB10	4.66	10.34	10.32
NYCaB35	5.35	9.09	9.29
NYCaB75	5.74	9.37	9.99
rms error = 4%			

half of that for NYAB crystal, and a quarter of that for Nd:YCOB crystal.<sup>21</sup> It is generally accepted that the  $\Omega_2$  parameter is an indicator of the metal–ligand bond covalence whereas the dimension of  $\Omega_6$  is related to the rigidity of the host. Following these premises, the fact that  $\Omega_2$  is higher for the NYCaB100x glasses than, for instance, for Nd<sup>3+</sup>-doped YAIB (Ref. 9) and Bi<sub>2</sub>O<sub>3</sub>–B<sub>2</sub>O<sub>3</sub> (Ref. 30) glasses is consistent with a higher asymmetry of the ligand field around the Nd<sup>3+</sup> ions which can, in principle, entail higher M–O orbital superposition. The latter, implies in extended relaxation of selection rules and consequently higher transition probabilities, which would explain the relatively shorter radiative lifetime values of NYCaB100x as compared to Nd:YAIB, for instance. This interpretation however, should not be viewed as a definite one since major structural differences in these systems might play a role. In the case of YAIB, it is known that Nd<sup>3+</sup> ions can occupy solely Y<sup>3+</sup> environments,<sup>11</sup> but for the YCaB glasses, in which Ca<sup>2+</sup> also substitutes for Y<sup>3+</sup>, the analysis of the far infrared reflectivity spectra has shown the possibility of different Ca<sup>2+</sup> occupational environments<sup>10</sup> similar to the case of binary CaO–B<sub>2</sub>O<sub>3</sub> glasses and crystals.<sup>29</sup> Structural investigations of NYCaB100x by high resolution solid

TABLE IV. Radiative transition rates and branching ratios for NYCaB100x glasses.

Sample	Transition <sup>4</sup> F <sub>3/2</sub> →	$\nu$ (cm <sup>-1</sup> )	Radiative rate (s <sup>-1</sup> )	$\beta$
NYCaB10	<sup>4</sup> I <sub>9/2</sub>	11 111.11	2920.48	0.414
	<sup>4</sup> I <sub>11/2</sub>	9442.87	3475.72	0.493
	<sup>4</sup> I <sub>13/2</sub>	7490.64	659.21	0.093
			A <sub>rad</sub> = 7055.41	
NYCaB35	<sup>4</sup> I <sub>9/2</sub>	11 111.11	2578.79	0.411
	<sup>4</sup> I <sub>11/2</sub>	9442.87	3108.57	0.495
	<sup>4</sup> I <sub>13/2</sub>	7490.64	593.12	0.094
			A <sub>rad</sub> = 6280.48	
NYCaB75	<sup>4</sup> I <sub>9/2</sub>	11 111.11	2679.95	0.405
	<sup>4</sup> I <sub>11/2</sub>	9442.87	3307.04	0.499
	<sup>4</sup> I <sub>13/2</sub>	7490.64	637.78	0.096
			A <sub>rad</sub> = 6624.77	

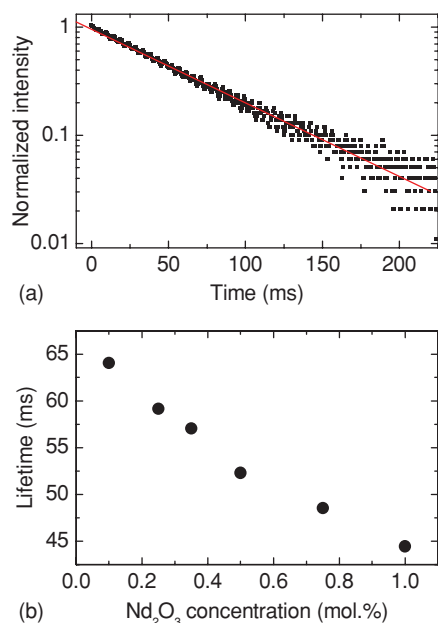


FIG. 3. (a) Luminescence intensity decay profile of the NYCaB25 glass ( $\lambda_{\text{exc}} = 800$  nm); (b)  $\text{Nd}_2\text{O}_3$  concentration dependence for  ${}^4\text{F}_{3/2}$  lifetime values in NYCaB100x glasses.

state NMR are currently being carried out and hopefully will provide further clarifications into such questions.

The experimental lifetime ( $\tau_{\text{exp}}$ ) values of the level  ${}^4\text{F}_{3/2}$  were determined from the first decay ( $e^{-1}$ ) of the luminescence intensity,  $I_{\text{lum}}(t)$ , and for comparison, using the equation  $\tau_{\text{eff}} = [\int I_{\text{lum}}(t)dt]/I_{\text{lum}}(0)$ , which presents an effective lifetime, where  $I_{\text{lum}}(0)$  is the luminescence intensity for  $t = 0$ . No appreciable difference, within  $\sim 4\%$ , was observed in the values obtained through both methods, indicating an exponential behavior to the decay of all the samples. Figure 3(a) shows a typical luminescence intensity decay spectrum for the NYCaB025 sample and Fig. 3(b) the dependence of the lifetime ( $\tau$ ) with the  $\text{Nd}_2\text{O}_3$  concentration. A typical behavior of  $\tau$  with the  $\text{Nd}_2\text{O}_3$  concentration is observed and attributed to interactions between  $\text{Nd}^{3+}$  ions as CRs and EM.

## B. Thermo-optical properties and fluorescence quantum efficiencies

The generation of heat and its effects on the thermo-optical properties of the NYCaB100x glasses were analyzed by the TL technique, in a similar way to our previous report on Nd:YAIB glasses.<sup>9</sup> The heat deposition is due to the absorption of light followed by nonradiative decays and it manifests itself through the establishment of temperature and refractive index gradients responsible for the lenslike behavior of the samples. This effect is analyzed in terms of the temperature coefficient of the optical path length change ( $ds/dT$ ). In the dual beam mode-mismatched TL configuration,<sup>20</sup> the propagation of a probe laser beam through the lenslike region results in a variation in its on-axis intensity which can be calculated using diffraction integral theory. The temporal evolution of the TL signal depends on the characteristic TL signal time  $t_c$ , which is related to the thermal diffusivity

( $D$ ) by  $D = w_e^2/4t_c$ . The latter relates to the thermal conductivity ( $K$ ) by  $K = \rho cD$ , where  $\rho$  is the sample density and  $c$  is the specific heat. The TL transient signal amplitude  $\theta$  is approximately the phase shift of the probe beam at  $r = 0$  and  $r = \sqrt{2}w_e$  induced by TL. When normalized by the absorbed power ( $P_{\text{abs}}$ ),  $\theta$  can be redefined as

$$\Theta = \frac{\theta}{P_{\text{abs}}} = -B\varphi, \quad (1)$$

where  $B = (K\lambda_p)^{-1}ds/dT$  is a constant that depends only on the host matrix characteristics and on the probe beam wavelength  $\lambda_p$ , and  $\varphi$  is the fraction of absorbed energy converted into heat. The latter, also called fractional thermal loading, is related to the fluorescence quantum efficiency as

$$\varphi = 1 - \eta \frac{\lambda_{\text{exc}}}{\langle \lambda_{\text{em}} \rangle}, \quad (2)$$

where  $\lambda_{\text{exc}}$  is the excitation wavelength and  $\langle \lambda_{\text{em}} \rangle$  is the average emission wavelength obtained with the relation  $\langle \lambda_{\text{em}} \rangle = \sum \lambda_i \beta_i$ , where  $\lambda_i$  is the wavelengths of emissions from the emitting level and  $\beta_i$  is the branching ratios related to such emissions probabilities. Thus, by knowing  $\theta$  and the host parameters contained in the constant  $B$ , one can, in principle, easily obtain  $\eta$ . One problem often encountered, however, is the lack of a reference and undoped sample for the determination of the host characteristics and/or their very low absorption coefficient which makes the TL signal hardly detectable and impedes the precise calculation of the absorbed power. In order to circumvent such problems in the study of NYCaB100x glasses, we employ the alternative method called normalized-lifetime thermal-lens.<sup>13,14</sup>

Figure 4(a) presents a characteristic TL transient signal for the NYCaB75 sample. The incident power for this transient was 30 mW and the fitting of the experimental

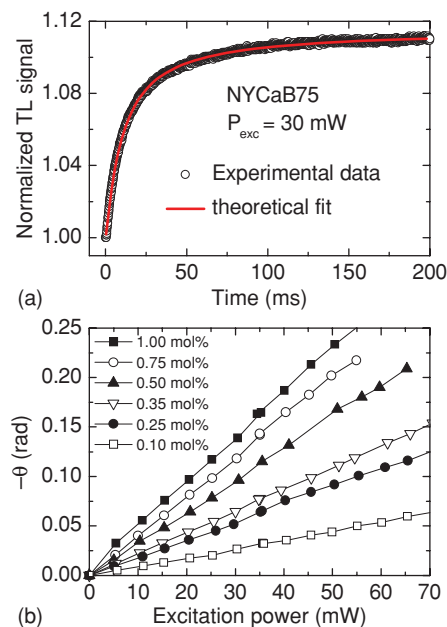


FIG. 4. (a) Representative thermal lens transient signal for NYCaB75 sample with  $\lambda_{\text{exc}} = 514.5$  nm and  $\lambda_p = 632.8$  nm; (b) Thermal lens phase shift ( $\theta$ ) against the excitation power for NYCaB100x glasses doped with different  $\text{Nd}_2\text{O}_3$  concentrations.

curve with the TL equation<sup>20</sup> (solid line) yields  $t_c = (1.18 \pm 0.11)$  ms and  $\theta = -(0.118 \pm 0.004)$  rad. The parameters  $t_c$  and  $\theta$  were obtained for all the samples as a function of pump power and doping concentration as shown in Fig. 4(b). In agreement with Eq. (1) a linear dependence of  $\theta$  with the excitation power  $P_e$  is observed. Having obtained  $t_c$ , the average value of  $D = (3.3 \pm 0.3) \times 10^{-3}$  cm<sup>2</sup>/s was calculated, and using this parameter together with  $\rho = (2.94 \pm 0.03)$  g/cm<sup>3</sup> and  $c = 0.727$  J/g K (this latter obtained from the Dulong–Petit relation), it was possible to calculate  $K = (7.1 \pm 0.7) \times 10^{-3}$  W/cm K. These values are somewhat lower than those determined for Nd:YAIB glasses [ $D = (4.1 \pm 0.3) \times 10^{-3}$  cm<sup>2</sup>/s and  $K = (10.6 \pm 0.8) \times 10^{-3}$  cm<sup>2</sup>/s],<sup>9</sup> but similar to those of the majority of the laser glasses.<sup>20</sup> Once the thermo-optical properties of the host YCaB were determined we proceeded to obtain  $\eta$  for all the doped samples.

Rigorously, the quantum efficiency is defined as the ratio of experimental to radiative lifetime values ( $\eta = \tau_{\text{exp}}/\tau_{\text{rad}}$ ). Since  $\tau_{\text{rad}}$  is independent of the Nd<sup>3+</sup> concentration, the lifetimes of two samples with concentrations  $N_0$  and  $N_x$ , for instance, can be compared as

$$\eta_{N_x} = \eta_{N_0} \frac{\tau_{N_x}}{\tau_{N_0}} = \eta_{N_0} \Gamma(N), \quad (3)$$

where

$$\Gamma(N) = \frac{\tau_{N_x}}{\tau_{N_0}}. \quad (4)$$

Combining Eqs. (1)–(3) the expression for the TL phase shift divided by the absorbed pump power can be rewritten as

$$\Theta = B \left[ 1 - \Gamma \eta_{N_0} \frac{\lambda_{\text{exc}}}{(\lambda_{\text{em}})} \right], \quad (5)$$

and the lifetime value  $\tau_{N_0}$  of a chosen sample can be used to normalize the lifetimes values  $\tau_{N_x}$  of the other samples in the set, so that through the behavior of  $\Theta$  versus  $\Gamma$  (see Fig. 5) the values of  $\eta_{N_0}$  can be determined through linear fitting, and further used in Eq. (3) to obtain  $\eta$  for the other samples. As the reference sample we chose the lowest doped one (0.1 mol%) for which it was found that  $\eta = 0.54$ . In addition, the value of  $B = (11.9 \pm 0.5) \text{ W}^{-1}$  was also

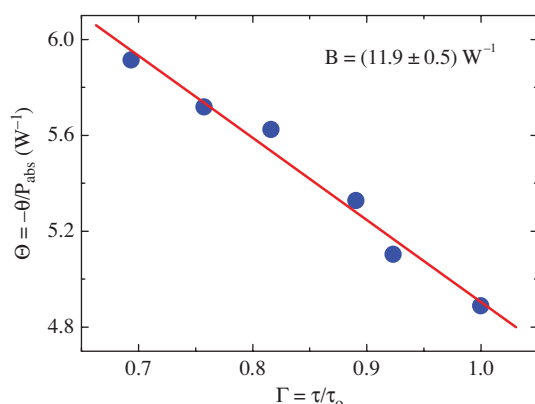


FIG. 5. (dots) Thermal lens phase shift divided by the absorbed pump power against the normalized lifetime  $\Gamma = \tau/\tau_0$  for the NYCaB samples. The solid line is the linear fit.

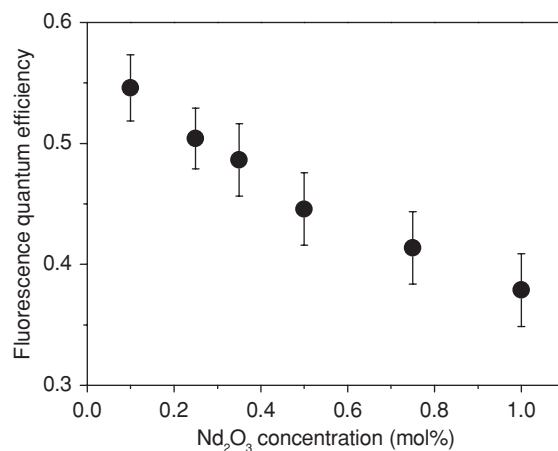


FIG. 6. Fluorescence quantum efficiency of NYCaB100x glasses as a function of Nd<sub>2</sub>O<sub>3</sub> concentration.

obtained from the fitting, allowing the calculation of  $ds/dT = (5.3 \pm 0.3) \times 10^{-6} \text{ K}^{-1}$ . Accordingly, this result is also lower than that of the Nd:YAIB glasses,<sup>9</sup> half of the aluminosilicate, larger than that of the phosphates, and fluorides as Zr-Ba-La-Al-Na (ZBLAN) glasses.<sup>13,20</sup> In resume, the  $D$ ,  $K$ , and  $ds/dT$  values are typical of laser glasses.

The dependence of  $\eta$  values with Nd<sub>2</sub>O<sub>3</sub> concentration is depicted in Fig. 6. It is found that these values are lower than unity but similar to those found in bismuth borate glasses,<sup>30</sup> where quasicontinuous laser operation was recently demonstrated.<sup>31</sup> Moreover, these values are higher than those for Nd<sup>3+</sup> doped GdCOB crystals ( $\eta = 14.8\%$  for  $2.2\text{--}8.8 \times 10^{19}$  Nd<sup>3+</sup> ions/cm<sup>3</sup>),<sup>26</sup> and considerably higher than those for Nd:YAIB glasses<sup>9</sup> and Nd<sup>3+</sup> doped YAB crystals<sup>28</sup> with comparable Nd<sup>3+</sup> concentrations. The relatively low value for the less doped sample is attributed to multiphonon decay due to high phonon energy of this matrix, which is from 1100 to 1400 cm<sup>-1</sup>. The reason for the decrease in  $\eta$  values with increasing concentration is, as earlier mentioned, the growing probability of the energy transfer processes by CR and EM, among Nd<sup>3+</sup> ions, followed by nonradiative decays (multiphonon in the case of CR). Therefore, it is useful to investigate such contributions.

### C. Energy transfer analysis

In general, the emission decay profiles of luminescent host–ion systems encompass radiative and nonradiative contributions. Particularly, the latter can lead to pronounced deviations from a single exponential pattern in lower or greater extent. Thus, profiles such as those in Fig. 3(a) are best described by the following equation:

$$I_{\text{lum}}(t) = I_0 \exp[-(A_{\text{rad}} + W_{\text{mp}})t - \bar{W}t - \gamma\sqrt{t}], \quad (6)$$

where  $A_{\text{rad}}$  and  $W_{\text{mp}}$  are the radiative and multiphonon decay rates, respectively, which are independent of ion concentration.  $\bar{W}$  accounts for the migration assisted cross relaxation energy transfer<sup>13,15,16</sup> and  $\exp(-\gamma\sqrt{t})$  is the classic Förster decay function,<sup>13,16,17,32</sup> also known as static disorder decay, accounting for direct cross relaxation. Although both  $\bar{W}$  and  $\gamma$

depend on concentration, only the latter leads to a deviation of the purely exponential behavior of the decay. This fact is usually attributed to the different distances between donors and acceptors leading to a decay rate that differs for each donor–acceptor pair. The resulting overall decay is then nonexponential, with an initial faster decay, due to sites with smaller separation between pairs. According to the Förster model,<sup>32</sup>  $\gamma$  is given by

$$\gamma = \frac{4}{3}\pi^{3/2}N_t\sqrt{C_{DA}}. \quad (7)$$

In 1983, Burshtein proposed the “hopping” model<sup>18</sup> to take into account the EM-assisted cross relaxation, through the following equation for  $\bar{W}$ :

$$\bar{W} = \pi \left( \frac{2\pi}{3} \right)^{5/2} \sqrt{C_{DA}C_{DD}N_t^2}. \quad (8)$$

In Eqs. (7) and (8),  $C_{DD}$  and  $C_{DA}$  stand for the microscopic energy transfer parameters that can be calculated using Dexter model of multipolar interactions.<sup>17</sup> The equations are intentionally written for the case of singly doped materials where the concentration of donor and acceptor ions,  $N_D$  and  $N_A$ , respectively, are equal to  $N_t$ , which corresponds to the total  $\text{Nd}^{3+}$  doping concentration. For this ion, the energy transfer processes can be well described on the basis of dipole–dipole interactions. The transitions involved in the CR related to  $C_{DA}$  are  ${}^4F_{3/2}$ ,  ${}^4I_{9/2} \rightarrow {}^4I_{15/2}$ ,  ${}^4I_{15/2}$  and/or  ${}^4F_{3/2}$ ,  ${}^4I_{9/2} \rightarrow {}^4I_{13/2}$ ,  ${}^4I_{15/2}$ ; and in the EM related to  $C_{DD}$  is  ${}^4F_{3/2}$ ,  ${}^4I_{9/2} \rightarrow {}^4I_{9/2}$ ,  ${}^4F_{3/2}$ .<sup>15,16</sup> The microscopic parameters can be obtained by using the spectral overlap integrals of donor ion emission ( $\sigma_D^{\text{em}}$ ) and acceptor ion absorption ( $\sigma_A^{\text{abs}}$ ) cross sections according to<sup>13,15,17</sup>

$$C_{DX} = \frac{3c}{8\pi^4 n_0^2} \int \sigma_D^{\text{em}}(\lambda)\sigma_X^{\text{abs}}(\lambda)d\lambda, \quad (9)$$

where X is equal to D or to A for the EM or CR mechanisms, respectively,  $c$  is the speed of light, and  $n_0$  is the refractive index of the medium. The calculation of  $C_{DD}$  is straightforward because energy migration is a resonant process and, therefore, the overlap integral has appreciable values. However, the CRs are nonresonant and the obtaining of the overlap integrals for the calculation of  $C_{DA}$  requires some data manipulation as to account for the phonon-assistance.<sup>17</sup> This procedure introduces further errors in the calculations, resulting in  $C_{DA}$  values that are usually reliable but not as much as that of  $C_{DD}$ .

The experimental data in Fig. 6 were also evaluated in terms of the microscopic energy transfer parameters by using Eq. (10) in agreement with Eq. (9):<sup>13,15,16</sup>

$$\eta(N_t, C_{DA}, C_{DD}) = \frac{A_{\text{rad}}}{I(0)} \int_0^\infty I(t)dt = \frac{A_r}{W_\infty} \times \{1 - \sqrt{\pi}x \exp(\chi^2)[1 - \text{erf}(x)]\}, \quad (10)$$

where  $W_\infty = A_{\text{rad}} + W_{\text{mp}} + \bar{W}$  and  $x = \gamma/2\sqrt{W_\infty}$ . The  $C_{DD} = (4.5 \pm 0.3) \times 10^{-39} \text{ cm}^6/\text{s}$  value was calculated according to Eq. (9). The error bar was estimated by calculating  $C_{DD}$  for two samples and using three methods to obtain the emission cross section.<sup>33,34</sup> After that, the  $C_{DD}$  value was used in

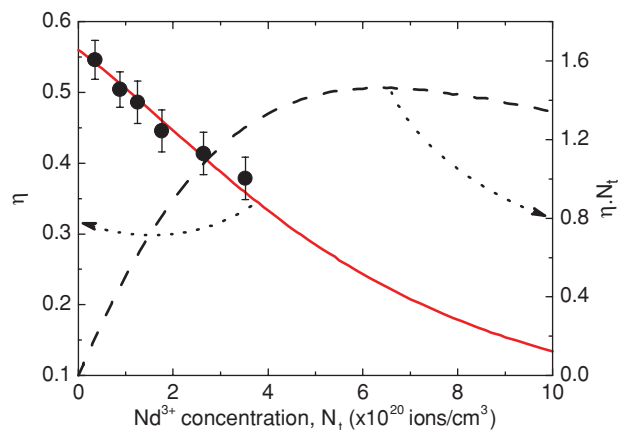


FIG. 7. Dependence on  $\text{Nd}^{3+}$  concentration of fluorescence quantum efficiency ( $\eta$ ) and figure of merit ( $\eta N_t$ ) for  ${}^4F_{3/2}$  level in NYCaB100x glass. Open symbols are  $\eta$  results obtained using the thermal lens technique; solid line is the fit of the open symbols using the Eq. (10); and dashed line is the figure of merit calculated with the solid line.

Eq. (10) by letting  $C_{DA}$  and  $W_{\text{mp}}$  to vary. The values obtained were  $C_{DA} = (2.8 \pm 0.7) \times 10^{-40} \text{ cm}^6/\text{s}$  and  $W_{\text{mp}}^{\text{exp}} = 6700 \text{ s}^{-1}$ . The multiphonon decay rate was also estimated using the experimental decay rate obtained for the lowest  $\text{Nd}^{3+}$  doped sample together with the radiative decay rate (obtained by JO theory) by means of the equation  $W_{\text{mp}}^{\text{cal}} = W_{\text{exp}} - W_{\text{rad}}$ , resulting in  $W_{\text{mp}}^{\text{cal}} = 8960 \text{ s}^{-1}$ . The difference between  $W_{\text{mp}}^{\text{cal}}$  and  $W_{\text{mp}}^{\text{exp}}$  of  $2260 \text{ s}^{-1}$ , however, must be attributed to the energy transfer rate in this lowest  $\text{Nd}^{3+}$  doped sample. The distribution of  $\eta$  as a function of concentration (dots) and the fit (solid line) with Eq. (10) is presented in Fig. 7. A little similar to the Nd:PLZT case,<sup>15</sup> the behavior of  $\eta$  versus  $\text{Nd}^{3+}$  concentration is strongly dependent on the  $C_{DA}$  value and slightly on the  $C_{DD}$  one, i.e., with a large variation of  $C_{DD}$  no appreciable change is observed in the fitting behavior, whereas a slight variations of  $C_{DA}$  varies appreciably the curve. This gives us clear indication that the highest influence on fluorescence quenching is mainly due to the CRs, although  $C_{DD}$  be almost one order of magnitude larger than  $C_{DA}$ . This way, by fixing the value of  $C_{DD}$  and letting  $C_{DA}$  and  $W_{\text{mp}}$  vary during the fitting procedure of the curve in Fig. 7, is a good method to obtain  $C_{DA}$ .

Since the reduction of  $\eta$  is balanced by the increase of the optical absorption coefficient with the increasing concentration, the figure of merit, defined as  $\eta N_t$  versus  $N_t$ , is a way to determine optimum concentrations for practical applications. Figure 7 also presents the figure of merit that shows a maximum around  $N_t = 6.0 \times 10^{20} \text{ Nd}^{3+} \text{ ions/cm}^3$ , concentration in which  $\eta = 0.24$ . This concentration is almost twice that for  $\text{Nd}^{3+}$ -doped yttrium aluminum garnet (Nd:YAG) system,<sup>35</sup> and the  $\eta = 0.24$  value is not so small when compared to other laser materials with similar  $\text{Nd}^{3+}$  concentration.<sup>9,28</sup> In other words, the NYCaB100x system has a much reduced concentration quenching effect, which put it as a prospective material for future applications.

#### IV. CONCLUSIONS

In summary, in this work we presented a complete and comprehensive study of the spectroscopic and thermo-optical properties of Nd<sup>3+</sup>-doped yttrium calcium borate glasses (Nd:YCaB) with composition  $x\text{Nd}_2\text{O}_3-(5-x)\text{Y}_2\text{O}_3-40\text{CaO}-55\text{B}_2\text{O}_3$  ( $0 \leq x \leq 1.0$  mol%). The spectroscopic properties obtained by luminescence and absorption measurements together with the Judd–Ofelt analysis testified the higher asymmetry of the ligand field around the Nd<sup>3+</sup> ions, which explains the relatively high radiative rate (low radiative lifetime) of the <sup>4</sup>F<sub>3/2</sub> Nd<sup>3+</sup> level in this system. The thermal lens technique was used to quantify the fluorescence quantum efficiency ( $\eta$ ) and the thermo-optical properties such as thermal diffusivity ( $D$ ) and conductivity ( $K$ ) and temperature coefficient of the optical path length change ( $ds/dT$ ). The values obtained for  $D$ ,  $K$ , and  $ds/dT$  are very similar to those of commercial laser glasses. A maximum  $\eta = 0.54$  for the lowest doped sample was found to be substantially higher than for other borates glasses and also crystal with comparable Nd<sup>3+</sup> content. The  $\eta$  dependence on the Nd<sup>3+</sup> concentration was analyzed in terms of energy transfer processes based on the Förster–Dexter model of multipolar ion–ion interactions. The obtained energy transfer microparameters  $C_{DD}$  and  $C_{DA}$  and the weak dependence of  $\eta$  on the Nd<sup>3+</sup> concentration with a high optimum Nd<sup>3+</sup> concentration, as indicated by the figure of merit, put this system as a strong candidate for photonics applications.

#### ACKNOWLEDGMENTS

The authors are thankful to the Brazilian agencies CAPES, FAPESP (Grant No. 04/00093–0), CNPq, FINEP, and FAPEAL and to the Brazil–France CAPES–COFECUB (Grant No. 455/04) agreement for the financial support of this work. The research of D. R. S. Santos is supported by undergraduate studentships from PIBIC/CNPq and those of W. F. Silva and W. Q. Santos by graduate studentships from CAPES and CAPES/FAPEAL (Project No. PEB-2009–03-015 (04)), respectively.

- <sup>1</sup>P. Becker, *Adv. Mater.* **10**, 979 (1998); D. Jaque, J. Capmany, and J. Garcia-Solé, *Appl. Phys. Lett.* **74**, 1788 (1999); P. Dekker and J. M. Dawes, *Opt. Express* **12**, 5922 (2004); P. Segonds, B. Boulanger, B. Menaert, J. Zaccaro, J. P. Salvestrini, M. D. Fontana, R. Moncorgé, F. Poree, G. Gadret, J. Mangin, A. Brenier, G. Boulon, G. Aka, and D. Pelenc, *Opt. Mater.* **29**, 975 (2007); A. Brenier, D. Jaque, and A. Majchrowski, *Opt. Mater.* **28**, 310 (2006).
- <sup>2</sup>P. Segonds, S. Joly, B. Boulanger, Y. Petit, C. Félix, B. Ménaert, and G. Aka, *J. Opt. Soc. Am. B* **26**, 750 (2009).
- <sup>3</sup>O. H. Heckl, C. Kränkel, C. R. E. Baer, and C. J. Saraceno, *Opt. Express* **18**, 19202 (2010).
- <sup>4</sup>M. Richardson, D. Hammons, J. Eichenholz, B. H. T. Chai, Q. Ye, W. K. Jang, and L. Shah, *J. Kor. Phys. Soc.* **37**, 633 (2000).
- <sup>5</sup>V. Petrov, X. Mateos, A. Schmidt, S. Rivier, U. Griebner, H. Zhang, J. Wang, J. Li, and J. Liu, *Laser Phys.* **20**, 1085 (2010); S. Rivier, U. Griebner, V. Petrov, H. Zhang, J. Li, J. Wang, and J. Liu, *Appl. Phys. B: Lasers Opt.* **93**, 753 (2008).
- <sup>6</sup>J. Bartschke, K.-J. Boller, R. Wallenstein, I. V. Klimov, V. B. Tsvetkov, and I. A. Shcherbakov, *J. Opt. Soc. Am. B* **14**, 3452 (1997); J. Eichenholz, H. T.

- B. Chai, Q. Ye, M. Richardson, and D. A. Hammons, U.S. patent 6,185,236 (6 February 2001).
- <sup>7</sup>B. H. T. Chai, D. A. Hammons, J. M. Eichenholz, Q. Ye, W. K. Jang, L. Shah, G. M. Luntz, M. Richardson, and H. Qiu, “Lasing, second harmonic conversion and self-frequency doubling of Yb:YCOB (Yb:YCa<sub>4</sub>B<sub>3</sub>O<sub>10</sub>),” in *Advanced Solid State Lasers*, OSA Trends in Optics and Photonics Series Vol. 19, edited by W. R. Bosenberg and M. M. Fejer (Optical Society of America, Washington, D.C., 1998), pp. 59–61.
- <sup>8</sup>I. N. Chakraborty, H. L. Rutz, and D. E. Day, *J. Non-Crystal. Sol.* **84**, 86 (1986); H. L. Rutz, D. E. Day, and C. F. Spencer, *J. Am. Ceram. Soc.* **73**, 1788 (1990); J. Rocherulle, *J. Mater. Sci. Lett.* **22**, 1127 (2003); N. Hemono, J. Rocherulle, M. Le Floch and B. Bureau, *J. Mater. Sci.* **41**, 445 (2006).
- <sup>9</sup>C. N. Santos, D. Mohr, W. F. Silva, A. S. S. de Camargo, H. Eckert, M. S. Li, M. V. D. Vermelho, A. C. Hernandez, A. Ibanez, and C. Jacinto, *J. Appl. Phys.* **106**, 023512 (2009).
- <sup>10</sup>C. N. Santos, D. S. Meneses, P. Echegut, D. R. Neuville, A. C. Hernandez, and A. Ibanez, *Appl. Phys. Lett.* **94**, 151901 (2009).
- <sup>11</sup>H. Deters, A. S. S. de Camargo, C. N. Santos, C. R. Ferrari, A. C. Hernandez, A. Ibanez, M. T. Rinke, and H. Eckert, *J. Phys. Chem. C* **113**, 16216 (2009).
- <sup>12</sup>H. Deters, A. S. S. de Camargo, C. N. Santos, and H. Eckert, *J. Phys. Chem. C* **114**, 14618 (2010).
- <sup>13</sup>C. Jacinto, S. L. Oliveira, L. A. O. Nunes, J. D. Myers, M. J. Myers, and T. Catunda, *Phys. Rev. B* **73**, 125107 (2006).
- <sup>14</sup>C. Jacinto, S. L. Oliveira, L. A. O. Nunes, T. Catunda, and M. J. V. Bell, *Appl. Phys. Lett.* **86**, 071911 (2005).
- <sup>15</sup>A. S. S. de Camargo, C. Jacinto, L. A. O. Nunes, T. Catunda, D. Garcia, E. R. Botero, and J. A. Eiras, *J. Appl. Phys.* **101**, 053111 (2007).
- <sup>16</sup>J. A. Caird, A. J. Ramponi, and P. R. Staver, *J. Opt. Soc. Am. B* **8**, 1391 (1991).
- <sup>17</sup>T. Förster, *Ann. Phys. (N.Y.)* **2**, 55 (1948); D. L. Dexter, *J. Chem. Phys.* **21**, 836 (1953); L. V. G. Tarelho, L. Gomes, and I. M. Ranieri, *Phys. Rev. B* **56**, 14344 (1997).
- <sup>18</sup>A. I. Burshtein, *Sov. Phys. JETP* **35**, 882 (1972).
- <sup>19</sup>E. M. Yoshimura, C. N. Santos, A. Ibanez, and A. C. Hernandez, *Opt. Mater.* **31**, 795 (2009).
- <sup>20</sup>C. Jacinto, D. N. Messias, A. A. Andrade, S. M. Lima, M. L. Baesso, and T. Catunda, *J. Non-Cryst. Solids* **352**, 3582 (2006); J. Shen, R. D. Lowe, and R. D. Snook, *Chem. Phys.* **165**, 385 (1992).
- <sup>21</sup>L. X. Li, M. Guo, H. D. Jiang, X. B. Hu, Z. S. Shao, J. Y. Wang, J. Q. Wei, H. R. Xia, Y. G. Liu, and M. H. Jiang, *Cryst. Res. Technol.* **35**, 1361 (2000).
- <sup>22</sup>Y. Chen, Y. Huang, M. Huang, R. Chen, and Z. Luo, *Opt. Mater.* **25**, 271 (2004).
- <sup>23</sup>K. Terashima, S. Tamura, S.-H. Kim, and T. Yoko, *J. Am. Ceram. Soc.* **80**, 2903 (1997).
- <sup>24</sup>A. Brenier, Y. Wu, P. Fu, R. Guo, and F. Jing, *J. Appl. Phys.* **98**, 123528 (2005).
- <sup>25</sup>A. Lupei, G. Aka, E. Antic-Fidancev, B. Viana, D. Vivien, and P. Aschehoug, *J. Phys.: Condens. Matter* **14**, 1107 (2002).
- <sup>26</sup>A. Lupei, E. Antic-Fidancev, G. Aka, D. Vivien, P. Aschehoug, Ph. Goldner, F. Pellé, and L. Gheorghie, *Phys. Rev. B* **65**, 224518 (2002).
- <sup>27</sup>B. R. Judd, *Phys. Rev.* **127**, 750 (1962); G. S. Ofelt, *J. Chem. Phys.* **37**, 511 (1962).
- <sup>28</sup>D. Jaque, J. Capmany, Z. D. Luo, and J. Garcia-Solé, *J. Phys. Condens. Matter* **9**, 9715 (1997).
- <sup>29</sup>Y. D. Yiannopoulos, G. D. Chryssikos, and E. I. Kamitsos, *Phys. Chem. Glasses* **42**, 164 (2001).
- <sup>30</sup>Y. Chen, Y. Huang, M. Huang, R. Chen, and Z. Luo, *J. Am. Ceram. Soc.* **88**, 19 (2005).
- <sup>31</sup>Y. J. Chen, X. H. Gong, Y. F. Lin, Z. D. Luo, and Y. D. Huang, *Opt. Mater.* **33**, 71 (2010).
- <sup>32</sup>T. Förster, *Z. Naturforsch. B* **4(a)**, 321 (1949).
- <sup>33</sup>A. S. S. de Camargo, C. Jacinto, T. Catunda, L. A. O. Nunes, D. Garcia, and J. A. Eiras, *J. Opt. Soc. Am. B* **23**, 2097 (2006).
- <sup>34</sup>A. S. S. de Camargo, Ph.d. Dissertation, (Instituto de Física de São Carlos-Universidade de São Paulo, 2003).
- <sup>35</sup>V. Lupei, A. Lupei, S. Georgescu, T. Taira, Y. Sato, and A. Ikesue, *Phys. Rev. B* **64**, 092102 (2001).